

## Neprilysin: An Enzyme Candidate to Slow the Progression of Alzheimer's Disease

Salim S. El-Amouri,<sup>\*†</sup> Hong Zhu,<sup>†</sup> Jin Yu,<sup>†</sup>  
Robert Marr,<sup>‡</sup> Inder M. Verma,<sup>‡</sup>  
and Mark S. Kindy<sup>\*†§</sup>

From the Departments of Molecular and Cellular Biochemistry,<sup>\*</sup> and Neurosciences,<sup>†</sup> Medical University of South Carolina, Charleston, South Carolina; the Ralph H. Johnson Veteran's Administration Medical Center,<sup>§</sup> Charleston, South Carolina; and the Laboratory of Genetics,<sup>‡</sup> The Salk Institute for Biological Studies, La Jolla, California

**It is well established that the extracellular deposition of amyloid  $\beta$  ( $A\beta$ ) peptide plays a central role in the development of Alzheimer's disease (AD). Therefore, either preventing the accumulation of  $A\beta$  peptide in the brain or accelerating its clearance may slow the rate of AD onset. Neprilysin (NEP) is the dominant  $A\beta$  peptide-degrading enzyme in the brain; NEP becomes inactivated and down-regulated during both the early stages of AD and aging. In this study, we investigated the effect of human (h)NEP gene transfer to the brain in a mouse model of AD before the development of amyloid plaques, and assessed how this treatment modality affected the accumulation of  $A\beta$  peptide and associated pathogenetic changes (eg, inflammation, oxidative stress, and memory impairment). Overexpression of hNEP for 4 months in young APP/ $\Delta$ PS1 double-transgenic mice resulted in reduction in  $A\beta$  peptide levels, attenuation of amyloid load, oxidative stress, and inflammation, and improved spatial orientation. Moreover, the overall reduction in amyloidosis and associated pathogenetic changes in the brain resulted in decreased memory impairment by ~50%. These data suggest that restoring NEP levels in the brain at the early stages of AD is an effective strategy to prevent or attenuate disease progression. (*Am J Pathol* 2008, 172:1342–1354; DOI: 10.2353/ajpath.2008.070620)**

Alzheimer's disease (AD) is a progressive neurodegenerative disorder characterized by a loss of neurons in discrete regions of the brain, particularly in the cortex and hippocampus.<sup>1,2</sup> The neuronal loss is accompanied by extracellular deposition of  $A\beta$  peptide in a form of senile

plaques and intracellular accumulation of neurofibrillary tangles made of a hyperphosphorylated form of the microtubule-associated protein tau.<sup>3</sup> Clinically, AD is characterized by a gradual decline in cognition, and changes in behavior and personality including difficulty in reasoning, disorientation, and language problems. The exact cause of AD is not yet clear, but it is widely assumed that accumulation and aggregation of  $A\beta$  peptide is the initial trigger for a complex, multistep cascade that includes gliosis, inflammatory changes, oxidative stress, neuritic/synaptic changes, tangle formation (microtubule changes), and neurotransmitter loss, leading to dementia.<sup>4</sup> Therefore, lowering the  $A\beta$  peptide levels in the brain would stop or delay the onset of AD. NEP as one of the  $A\beta$  peptide-degrading enzymes, has been reported to play a key role in regulating the level of  $A\beta$  peptide in the brain.<sup>5,6</sup>

NEP [neprilysin, previously called CD10 or common acute lymphoblastic leukemia antigen (CALLA)] is a type II membrane metalloendopeptidase composed of ~750 residues (~110 kDa) with an active site containing a zinc-binding motif (HEXXH) at the extracellular carboxyl terminal domain.<sup>7–10</sup> NEP is capable of degrading the monomeric and (possibly) the oligomeric forms of  $A\beta$  peptide.<sup>11,12</sup> In recent years several reports have indicated that the soluble (eg, oligomeric) forms of  $A\beta$  peptide play a significant role in memory impairment and AD,<sup>13–15</sup> however, it is noteworthy that the two types of  $A\beta$  peptide assembly [soluble (eg, monomers and oligomers) and insoluble (eg, fibrils)] exist in equilibrium.<sup>16</sup> This relationship means that affecting the formation and metabolism of one structure also can affect the other, and the end result will be either slowing or preventing the progression of the disease. Thus, a mechanism to control the degradable (monomeric) form of  $A\beta$  peptide by NEP might prove to be a major factor in regulating the initiation and progression of the disease. Moreover, a diverse line of evidence suggested that down-regulation of NEP at

Supported by the National Institutes of Health (grant AG019323 to M.S.K.) and the Veteran's Administration (Merit Review to M.S.K.).

Accepted for publication February 5, 2008.

Address reprint requests to Mark S. Kindy, Department of Neurosciences, Medical University of South Carolina, Basic Science Building, Room 403, 173 Ashley Ave., Charleston, SC 29425. E-mail: kindyms@ musc.edu.

the early stages of AD development,<sup>17-19</sup> accompanied with aging,<sup>19,20</sup> genetic deficiency (knockout),<sup>6</sup> or treatment with NEP in the inhibitors,<sup>21,22</sup> results in increasing the accumulation of A $\beta$  peptide in the brain and thus led to memory impairment. Therefore, increasing the expression or activity of NEP in the early phase of the disease may reverse or halt the disease onset.

In this study, we used lentiviral vectors as a gene delivery system to overexpress hNEP in the cortical/hippocampal area of a mouse model of AD before the development of amyloid plaques. This overexpression may be important in restoring the function of NEP, which in turn would enhance the clearance of A $\beta$  peptide, minimize the formation of A $\beta$  aggregates and amyloid plaques, and prevent the pathogenic changes in the brain.

## Materials and Methods

### Lentiviral Vector Production

Vector plasmids were constructed for the production of third generation lentiviral vectors. These vectors separately express the hNEP gene (Lenti-hNEP), or the green fluorescent protein (GFP) gene (Lenti-GFP, control), as described previously.<sup>23-25</sup> Briefly, HEK 293T cells were transfected with the vector and packaging plasmids, the supernatants were collected, and viruses were concentrated by ultracentrifugation. Viral titers were estimated by flow cytometry (see below).

### Flow Cytometry

HEK 293T cells were counted and plated on six-well plates before infection. Serial dilution of the lentivirus preparations were made in culture medium and used to infect the cultures by incubation with cells overnight in a volume of 500  $\mu$ l. On the next day, infected cells were washed with fresh medium and incubated for 3 more days to allow for the expression of the transgenes. The transduced cells were then detached from the culture plates with a buffer containing ethylenediaminetetraacetic acid, and washed twice with ice-cold phosphate-buffered saline (PBS) buffer. The pellets of cells infected with Lenti-hNEP were resuspended in 0.5 ml of PBS buffer containing 10  $\mu$ l of fluorescein isothiocyanate-conjugated mouse anti-human CD10 antibody (Chemicon International, Temecula, CA) and incubated for 1 hour at 4°C. Cells were then washed twice with ice-cold PBS and analyzed by flow cytometry. The pellets of cells transduced with Lenti-GFP were resuspended in 0.5 ml of ice-cold PBS and directly analyzed by flow cytometry. The percentage of positive cells expressing hNEP or GFP was used to determine the number of transducing units per ml according to the formula:

$$\frac{\text{Number of seeded cells at the time of infection} \times \text{\% of GFP or hNEP-positive cells} \times 1000}{\mu\text{l of lentiviral vectors per plate}}$$

### Transgenic Mice

A total of 38, 3-month-old transgenic mice were used for the studies. The mice expressed the mutant form of human presenilin-1 (DeltaE9) and the mutant form of the chimeric mouse/human amyloid precursor protein (APP695).<sup>26,27</sup> The mouse prion protein promoter directed the expression of both transgenes. The DeltaE9 mutation of the human presenilin-1 gene is a deletion of exon 9 and corresponds to a form associated with early-onset AD. The APP695 gene harbors the K595N/M596L (Swedish) AD-causing mutations. The coding sequence of mouse A $\beta$  peptide domain was humanized by replacing the three amino acids that differ between the two species with the human residues. These APP/ $\Delta$ PS1-Tg mice start developing amyloid plaques at ~3 to 4 months of age. These mice were on a C3H/HeJ\* C57BL/6J background.

### Wild-Type Mice

Ten 7-month-old wild-type (C57BL/6) mice were used in interleukin (IL)-6 enzyme-linked immunosorbent assays (ELISAs) and protein carbonyl content assays.

### Intracerebral Injections of Lentiviruses and Preparation of Brain Tissue

Two sets of APP/ $\Delta$ PS1-Tg mice were separately injected with ~3.0  $\mu$ l (~3.0  $\times$  10<sup>6</sup> transducing units/mouse) of Lenti-GFP (18 mice) or Lenti-hNEP (20 mice) into the right cortical/hippocampal area using a 5.0- $\mu$ l Hamilton syringe (0.25  $\mu$ l/minute) and stereotaxic frame (stereotaxic coordinates: anteroposterior, 1.2 mm; mediolateral, 2.0 mm; dorsoventral, 2.0 mm). Four months after the viral injection, animals were transcardially perfused under deep anesthesia with 1 $\times$  PBS and their brains removed for further analysis. The right brain hemispheres were immersion-fixed in 4% paraformaldehyde for 24 hours, followed by immersion in 4% paraformaldehyde containing 30% sucrose for 2 to 3 days. After fixation, the right brain hemispheres were frozen in OCT medium and sectioned with a cryostat to obtain 30- $\mu$ m frozen sections for immunohistochemical analysis. The left brain hemispheres were frozen as quickly as possible and used to quantitate the levels of A $\beta$  peptide (A $\beta$ <sub>1-40</sub> and A $\beta$ <sub>1-42</sub>), IL-6, and protein carbonyl content.

### Immunohistochemistry Staining

Cryosections of the right brain hemispheres were washed three times (5 minutes/wash) with Tris-buffered saline (TBS) (pH 7.4) buffer, followed by washing one time with 0.1% Triton X-100-TBS buffer for 5 minutes. Sections were then incubated in 3% H<sub>2</sub>O<sub>2</sub> and TBS buffer for 30 minutes at room temperature to eliminate endogenous peroxidase activity. After 1 hour of blocking with 5.0% serum (horse or goat), the sections were incubated overnight with primary antibodies. Primary antibodies and dilutions were: hNEP, mouse anti-human CD10 antibody (1:100 dilution, SS2/36; DAKO, Carpinteria, CA); A $\beta$  pep-

tide, mouse anti-human A $\beta$  peptide antibody (1:500 dilution, 10D5; Elan Pharmaceuticals, San Francisco, CA); CD68-positive microglia, anti-mouse CD68 antibody (1:400 dilution, KP1; Abcam, Cambridge, MA); 3-nitrotyrosine (3-NT), rat anti-3-NT (1:500 dilution, 1A6; Upstate, Charlottesville, VA); GFAP-positive astrocytes (1:200 dilution, 2E1; BD Biosciences, San Jose, CA); Iba-1-positive microglia, rabbit anti-mouse Iba-1 antibody (1:500 dilution; Wako Chemicals, Richmond, VA). The next day, sections were washed three times (5 minutes/wash) with 0.1% Triton X-100 and TBS buffer to remove excess primary antibody. Thereafter, primary antibodies were detected using horseradish peroxidase-conjugated mouse or rat IgG Vectastain ABC kit and DAB/substrate reagents (Vector Laboratories, Burlingame, CA) according to the manufacturer's instructions.

### *A $\beta$ Peptide and IL-6 ELISA Assays*

Left brain hemispheres were weighted and homogenized with 4 vol of PBS buffer (125 mg/ml) containing complete protease inhibitor cocktail (Sigma-Aldrich, St. Louis, MO). Half the volume of the homogenates were mixed with 8.2 mol/L guanidine-HCl (pH 7.4) to a final concentration of 5 mol/L for 4 hours at room temperature. Guanidine extracts were then diluted 1:50 in BSAT-DPBS buffer (Dulbecco's phosphate buffered saline with 5% bovine serum albumin, 0.03% Tween 20, and 1 $\times$  protease inhibitor cocktail), mixed, and spun at 16,000  $\times$  g for 20 minutes at 4°C. The supernatants were used to measure A $\beta$  peptide levels by human A $\beta_{1-40}$  and A $\beta_{1-42}$  ELISA kits (Biosource International, Camarillo, CA). The remainder of the brain homogenates was subsequently centrifuged at 12,000  $\times$  g for 20 minutes at 4°C. The supernatant was then collected and total protein was determined by the BCA method (Pierce Biotechnology, Rockford, IL). IL-6 levels were measured with a mouse IL-6 ELISA kit (Biosource International).

### *Protein Carbonyl Content*

Protein carbonyl content was determined by the Oxyblot kit (Biosource International) and Western blot assay. Briefly, samples (20  $\mu$ g proteins/supernatant) were derivatized by 10 mmol/L of 2,4-dinitrophenylhydrazine (DNPH) to 2, 4-dinitrophenylhydrazone (DNP). The derivatized proteins (DNP proteins) were analyzed by Western blot using the rabbit primary antibody against the DNP moiety of the proteins, followed by secondary antibody (horseradish peroxidase-conjugated goat anti-rabbit IgG), and visualization by enhanced chemiluminescence reagents (Amersham Bioscience, Piscataway, NJ).

### *Coomassie Brilliant Blue Staining*

Duplicate samples used to measure protein-carbonyl content were analyzed on sodium dodecyl sulfate-polyacrylamide gel electrophoresis and stained to control for loading differences between samples. These duplicate

gels were stained with Coomassie brilliant blue solution [0.025% Coomassie brilliant blue (Sigma-Aldrich), 40% methanol, 7% acetic acid] for 45 minutes and destained with 40% methanol and 7% acetic acid overnight.

### *Thioflavin-S Staining*

Cryosections of mouse brains stained with anti-3NT antibody were mounted on glass slide and incubated with 1% thioflavin-S (Sigma, St. Louis, MO) in 70% ethanol for 20 minutes; sections were then rinsed with 70%, 95%, and 100% ethanol. Thioflavin-S was visualized by confocal microscopy using a specific filter set (excitation, 405 to 445 nm; emission, 515 to 565 nm).

### *Morris Water Maze Test*

A circular water tank, made from aluminum (diameter, 100 cm; height, 40 cm) was filled to a depth of 25 cm with water (23°C) and rendered opaque by the addition of a small amount of nontoxic white powder. Four positions around the edge of the tank were arbitrarily designated north (N), south (S), east (E), and west (W); to provide four alternative start positions and define the division of the tank into four quadrants: NE, SE, SW, and NW. A square white Perspex escape platform (10  $\times$  10  $\times$  2 cm) was submerged 1.0 cm below the water surface and placed at the midpoint of NE quadrant. The platform was invisible to the mice. Four visible cues to assist the mice for spatial analysis were placed outside the wall of the pool. A video camera, connected to SMART video tracking system (San Diego Instruments, San Diego, CA), was fixed 1.6 m above the center of the swim tank, and all swimming trials were recorded for further analysis. Four months after viral injection, each APP/ $\Delta$ PS1-Tg mouse overexpressing hNEP or GFP was trained for 4 consecutive days to reach the platform from the four different starting points. Starting points were randomized every day during the 4 day trials. Each mouse was placed gently in the pool facing the tank wall. Every mouse was allowed to swim and reach the platform within 60 seconds (spatial learning). If the mouse reached the platform, it was allowed to stay on the platform for another 30 seconds. If the mouse failed to reach the platform, it was gently placed on the platform for 30 seconds. Before the next trial, each mouse was allowed to rest for 10 minutes. On the day after the last training session, the platform was removed, and each mouse was allowed to search for the platform within 60 seconds (memory retention). To compare the spatial learning and memory retention between the mice overexpressing hNEP or GFP, the escape latency and distance taken by the mice to reach the platform were measured on the 4th day before removing the platform. In addition, the percent time that each mouse spent in the NE quadrant and in the outer annular were measured on the last day in absence of the platform.

## Statistical Analysis

Results were expressed as mean  $\pm$  SEM. Multiple comparison of amyloid plaque numbers, concentration of A $\beta$  peptide (A $\beta$ <sub>1-40</sub> and A $\beta$ <sub>1-42</sub>) and IL-6 were performed by one-way analysis of variance followed by Tukey's multiple comparison tests. A two-way analysis of variance was used to evaluate the differences in number of CD68-positive microglia and GFAP-positive astrocytes in the hippocampus and cortex areas. Statistical analysis of the Morris water maze test was performed using a two-way analysis of variance. In all comparisons, a difference with a *P* value less than 0.05 was considered statistically significant.

## Results

### Expression of hNEP in the Brain Attenuates the Level of A $\beta$ Peptide

The APP/ $\Delta$ PS1-Tg mice used in this study began to exhibit an increased level of A $\beta$  peptide and deposition of amyloid plaques in the cortex at the age of 3 months (Figure 1, A–D). The increase of amyloid load in the brain was associated with small numbers of GFAP-positive astrocytes in the cortex area, along the hippocampus region (data not shown), without signs of microgliosis. Therefore, 3-month-old APP/ $\Delta$ PS1-Tg mice exhibit early stages of AD-like pathology and were selected for testing lentiviral gene therapy. Moreover, these mice show a dramatic increase in amyloid load and memory impairment by 6 to 8 months,<sup>27,28</sup> at which time the effect of hNEP gene therapy could be measured.

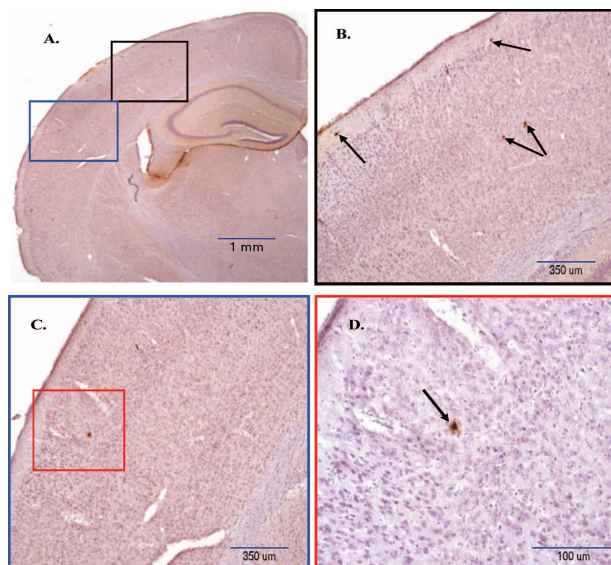


**Figure 1.** Amyloid plaque deposition in the brain of 3-month-old APP/ $\Delta$ PS1-Tg mice. Brain sections of 3-month-old APP/ $\Delta$ PS1-Tg mice were immunostained with anti-A $\beta$  peptide antibody (10D5) to detect the amyloid plaque deposition. **A:** Right brain hemisphere was examined in different areas and under increasing magnification (**B–D**) (**black, blue, and red boxes**) as indicated in the figure. **Arrows** point to the amyloid plaques in the cortex.

Three-month-old APP/ $\Delta$ PS1-Tg mice were injected with 3  $\mu$ l (1  $\mu$ l =  $9.0 \times 10^5$  transducing units) of Lenti-hNEP or Lenti-GFP in the right hippocampal/cortex area (Lenti-hNEP, *n* = 20; Lenti-GFP, *n* = 18). Age-matched, untreated transgenic mice were also used in these experiments. Four months later, all mice were sacrificed and sections of the right brain hemisphere were subjected to immunohistochemistry. Sections were stained with GFP or hNEP-specific antibodies (Figure 2). As shown in the figure, mice injected with Lenti-GFP had no or low detectable levels of NEP expression (Figure 2L) comparable to that seen in control animals (Figure 2, D and H). However, mice injected with Lenti-hNEP had significant overexpression of the protein that appeared mainly in the neurons and occasionally in glial cells (Figure 2T and data not shown). hNEP expression was observed around and distally to the site of injection. The expression of both proteins (GFP and hNEP) was restricted to the cortex area with occasional, weak expression in the hippocampus region. The expression in the cortex extended to  $\sim$ 2.0 mm on both sides from the center of the injection site. Western blot analysis showed a threefold increase in NEP expression in the hNEP mice (Figure 3).

To evaluate the effect of hNEP overexpression on the A $\beta$  peptide levels in the brain, we measured the levels of A $\beta$ <sub>1-40</sub> and A $\beta$ <sub>1-42</sub> peptides and the number of amyloid plaques. Immunostaining of 10 random cryostat sections (each spaced by at least five unused sections to prevent double counts) of each right brain hemisphere was performed on APP/ $\Delta$ PS1-Tg mice overexpressing hNEP or GFP (Figure 4). As seen in Figure 4, A and B, the number of amyloid plaques was reduced 4 months after the Lenti-hNEP injection. The overexpression of hNEP correlated with a 50% decrease in the number of amyloid plaques (control,  $279 \pm 32.6$ ; GFP,  $290 \pm 56.6$ ; NEP,  $145 \pm 29.6$ ) in the right brain hemispheres (Figure 4C). In addition, the concentrations of A $\beta$  peptide (A $\beta$ <sub>1-40</sub> and A $\beta$ <sub>1-42</sub>) in the brain (left hemisphere) were analyzed by ELISA (Figure 4, D and E; and Table 1). The guanidine-extractable A $\beta$ <sub>1-40</sub> and A $\beta$ <sub>1-42</sub> peptides in the brain were decreased by 33% and 40% in the brain, respectively.

### A $\beta$ Peptide Levels and Inflammation in the Brain

To investigate whether there were any measurable effects on the brain of treated APP/ $\Delta$ PS1-Tg mice as a result of amyloid load attenuation, we performed immunohistochemical staining on the right brain hemisphere sections obtained from mice overexpressing hNEP or GFP. The density of CD68-positive microglial cells were reduced in mouse brains overexpressing hNEP (Figure 5, A–C) compared to mouse brains overexpressing GFP (Figure 5, D–F). We also stained the tissue with antibodies against Iba-1 (ionized binding calcium adapter molecule), which is a novel calcium-binding protein and is specifically expressed in microglia in the brain, and showed the same expression pattern as CD68 (Figure 6).<sup>29</sup> A quantitative analysis of CD68-positive microglia revealed that the number of cells was reduced to 53.8%

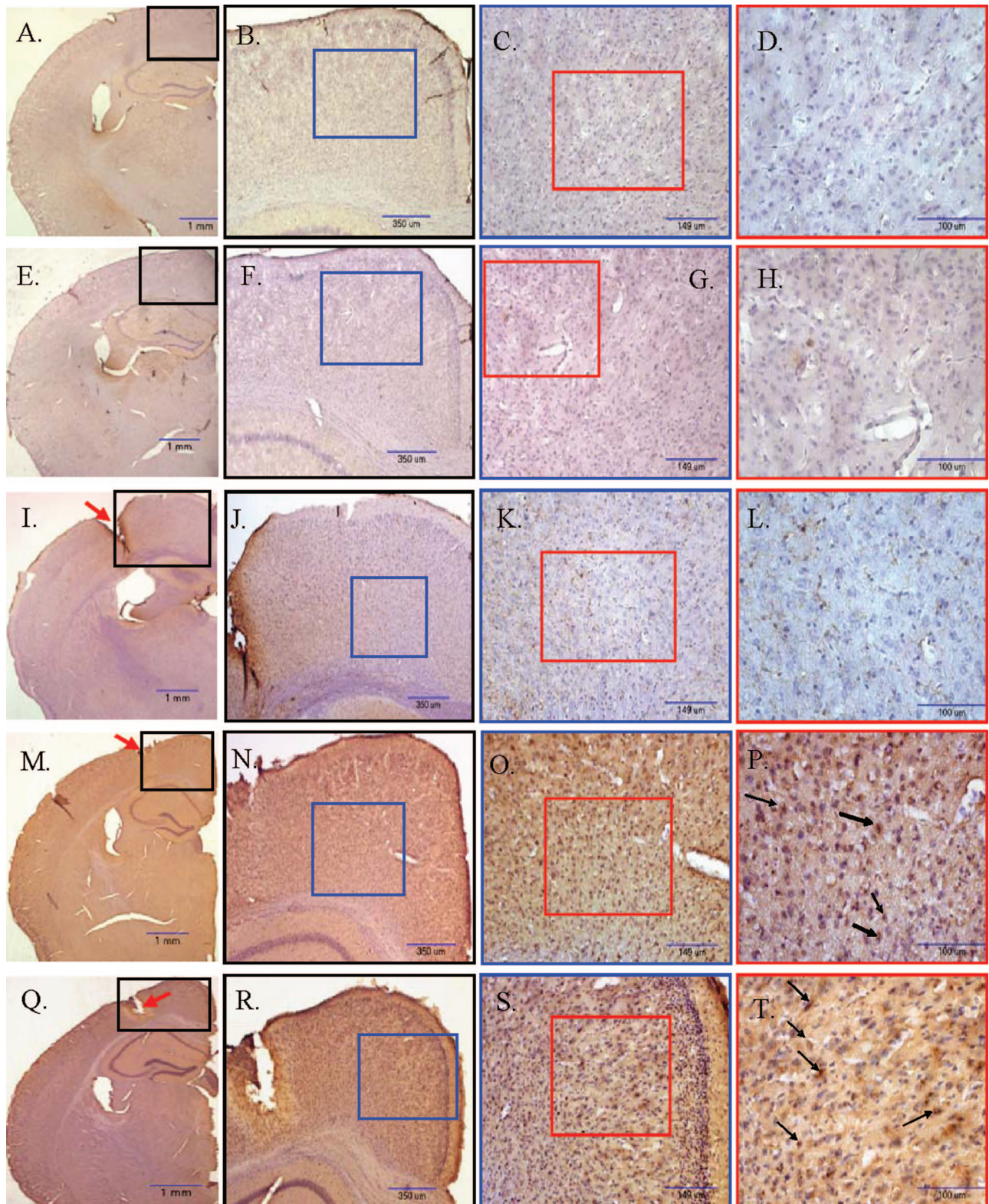


**Figure 2.** Expression of GFP and hNEP in the brain 4 months after viral injection of 3-month-old APP/ $\Delta$ PS1-Tg mice. **A–H:** Right brain hemisphere sections (30  $\mu$ m) of nontreated 8-month-old APP/ $\Delta$ PS1-Tg mice were IHC stained with antibodies against GFP (**A–D**) or hNEP (**E–H**). **I–L:** Sections of right brain hemisphere (around the injection site, **red arrow**) obtained from mice overexpressing GFP were immunostained with anti-hNEP antibody as a negative control. **M–P:** Sections of right brain hemisphere obtained from mice overexpressing GFP were immunostained with anti-GFP antibodies to detect GFP expression. **Q–T:** Sections of right brain hemisphere obtained from mice overexpressing hNEP were immunostained with anti-hNEP antibody to detect hNEP expression. **A, E, I, M,** and **Q** were examined at different magnification (**black, blue,** and **red boxes**) as indicated. **Black arrows** show examples of GFP (**P**-) and hNEP (**T**-) positive neurons.

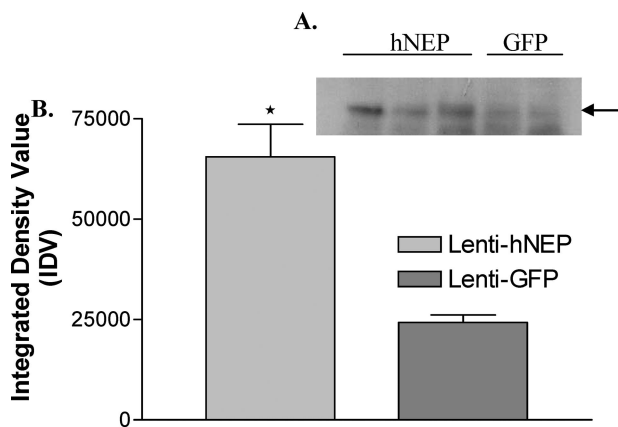


**Figure 3.** NEP expression in lentiviral injected animals. **A:** Western blot analysis was performed on brain tissue from mice injected with Lenti-hNEP (hNEP) or Lenti-GFP (GFP). Three hundred mg of brain tissue (around the injection site) was homogenized and 20  $\mu$ g of protein homogenates were immunoblotted with CD-10 antibody (1:100 dilution, Novocastra). Mice injected with Lenti-hNEP show an increase in NEP expression compared to Lenti-GFP mice. **Black arrow** indicates the  $\sim$ 110-kDa band of hNEP protein on Western blot. **B:** Densitometry measurements of developed NEP bands on Western blots were made using NIH image software (ImageJ1.36b) and assigned as arbitrary integrated density values (IDV) (\* $P = 0.0222$ ).

in the cortex areas (Figure 7A) ( $175.3 \pm 25.73$  versus  $379.8 \pm 70.30$ ) and 58.0% in the hippocampus areas (Figure 7B) ( $49.71 \pm 3.78$  versus  $118.6 \pm 17.04$ ) of mouse brains overexpressing hNEP compared to mouse brains overexpressing GFP. Similarly, the density of GFAP-positive astrocytes was reduced in mouse brains

overexpressing hNEP (Figure 5, G–I) compared to mouse brains overexpressing GFP (Figure 5, J–L). The number of GFAP-positive astrocytes was reduced by 60.1% in the cortex areas ( $334.3 \pm 64.3$  versus  $839.3 \pm 164.3$ ) (Figure 7C) and by 58.7% in the hippocampus areas ( $242.4 \pm 31.6$  versus  $587.3 \pm 71.0$ ) (Figure 7D) of mouse brains overexpressing hNEP compared to mouse brains overexpressing GFP. In addition, we measured by ELISA the levels of IL-6 (another indicator of inflammation) in the homogenates obtained from the left brain hemisphere of control and treated mice (Figure 7E).<sup>30</sup> APP/ $\Delta$ PS1-Tg mice (Tg) had a significant increase in IL-6 levels compared to the wild-type animals (Wt). Interestingly, the GFP injected APP/ $\Delta$ PS1-Tg mice (GFP) had an increase in IL-6 although this increase was not significant. However, the hNEP-injected APP/ $\Delta$ PS1-Tg mice had a significant reduction in IL-6 levels compared to untreated APP/ $\Delta$ PS1-Tg mice as well as to mice injected with GFP virus (Figure 7E, Table 2). The reductions in IL-6 levels were 33% compared to the untreated mice, and 54% compared to GFP-injected mice.

#### Reduction of A $\beta$ Peptide by hNEP Decreased Oxidative Stress

Next, we examined the oxidative stress level in mouse brains overexpressing hNEP or GFP by performing immunohistochemical staining for 3-nitrotyrosine (3-NT),

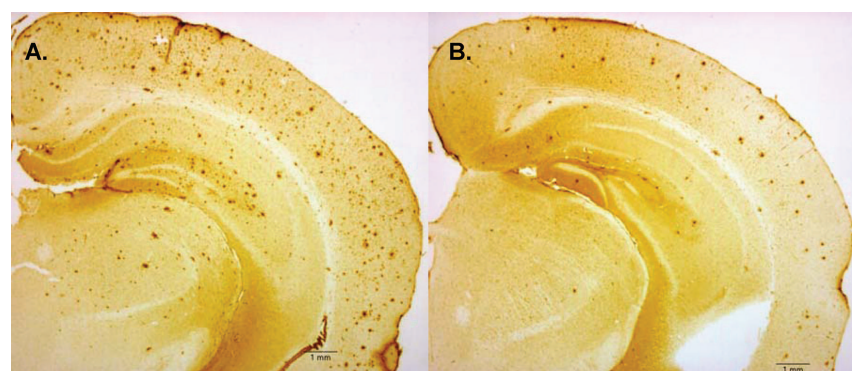


**Figure 4.** Level of amyloid load after 4 months of overexpressing GFP or hNEP in APP/ $\Delta$ PS1-Tg mouse brains. Right brain hemisphere sections obtained from mice injected with Lenti-GFP (**A**) or Lenti-hNEP (**B**) vectors were immunostained with mouse anti-human A $\beta$  peptide (clone 10D5) antibody to detect amyloid plaques. The number of amyloid plaques in the brain sections (10 sections per mouse) from each set of mice injected with Lenti-GFP or Lenti-hNEP vectors were counted and averaged (**C**). The left-brain hemisphere was examined for guanidine-extractable A $\beta$ <sub>1-40</sub> (**D**), and A $\beta$ <sub>1-42</sub> peptides (**E**). Tg-control: 7-month-old APP/ $\Delta$ PS1-Tg mice that were not injected with either lentiviral vectors (Lenti-hNEP or Lenti-GFP) were used as controls (\* $P < 0.0008$ , \*\* $P < 0.0001$ , \*\*\* $P = 0.0064$ ).

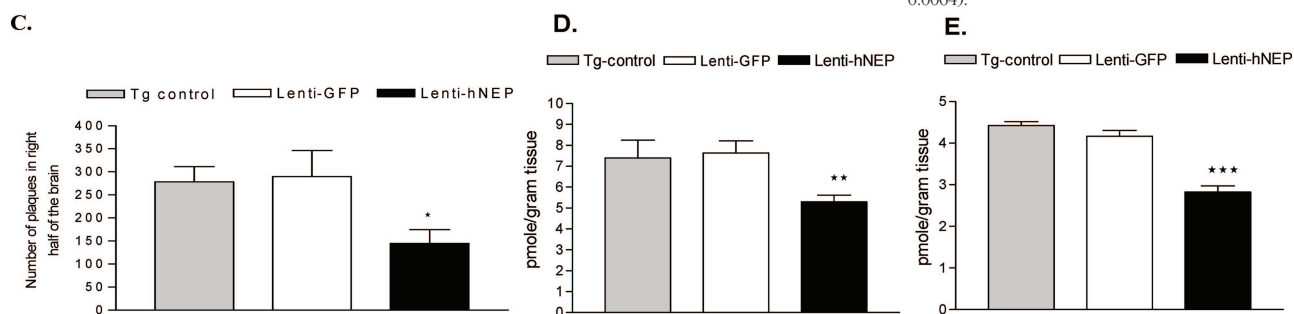


**Table 1.** A $\beta$  Peptide Levels in APP/ $\Delta$ PS1 Bitransgenic Mice Injected with Lentiviruses

	Control	GFP	NEP
A $\beta$ <sub>1-40</sub> (pmol/g)	7.395 $\pm$ 0.858	7.635 $\pm$ 0.580	5.292 $\pm$ 0.322
A $\beta$ <sub>1-42</sub> (pmol/g)	4.424 $\pm$ 0.089	4.168 $\pm$ 0.139	2.829 $\pm$ 0.144

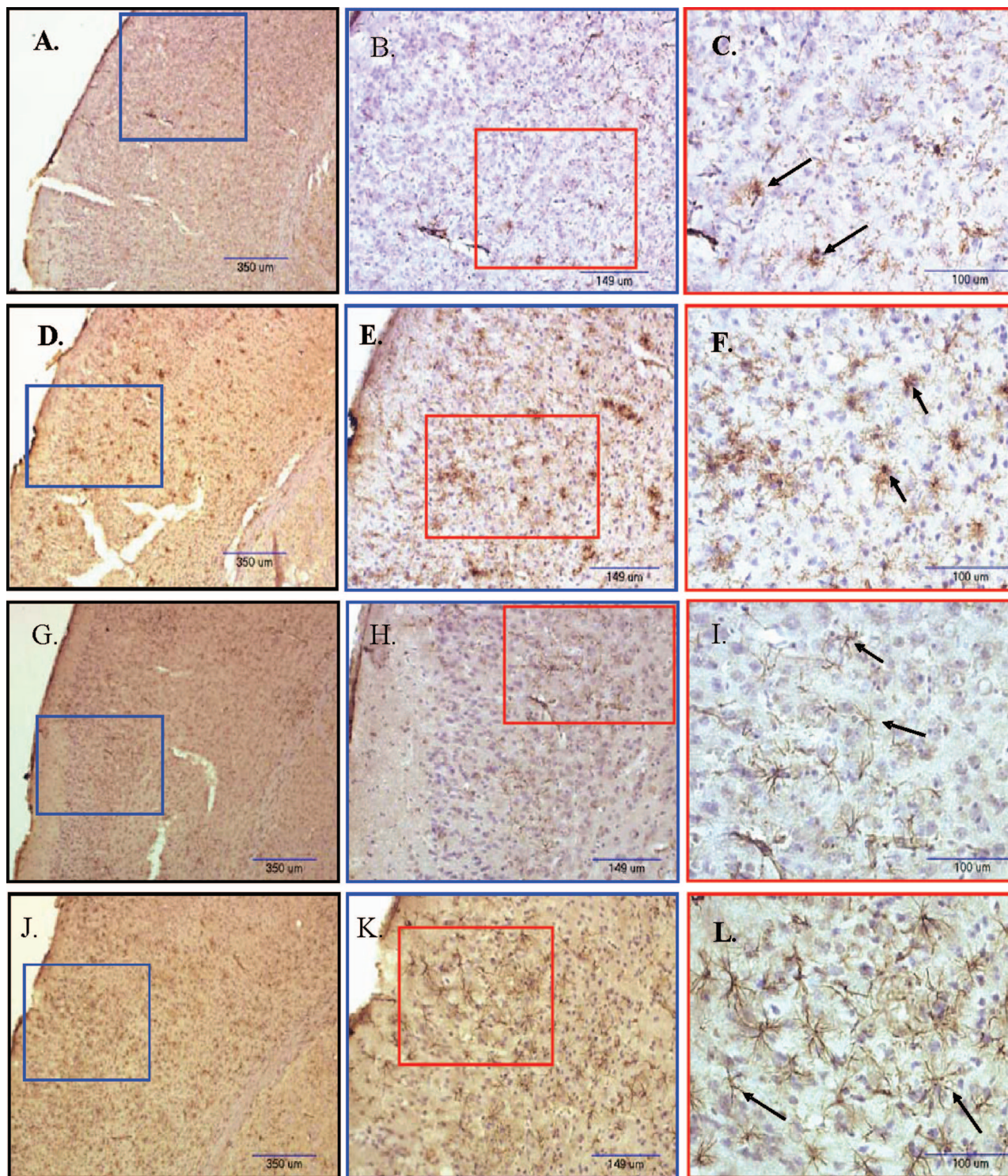


**Figure 5.** Density of activated microglia and astrocytes in APP/ $\Delta$ PS1-Tg mouse brain after 4 months of Lenti-GFP or -hNEP vector injection. **A–F:** Brain sections from APP/ $\Delta$ PS1-Tg mice overexpressing hNEP (**A–C**) or GFP (**D–F**) were immunostained with anti-mouse CD68 antibody to detect the distribution of activated microglial cells. **G–L:** Brain sections of APP/ $\Delta$ PS1-Tg mice overexpressing hNEP (**G–I**) or GFP (**J–L**) were immunostained with anti-mouse GFAP antibody to detect the distribution of activated astrocytes. The figures (**A**, **D**, **G**, and **J**) were examined at different magnification (**blue** and **red boxes**) as indicated. **Black arrows** in **C** and **F** show examples of CD68-activated microglia, whereas in **I** and **L** they indicate activated GFAP-positive astrocytes.

which is a biomarker of reactive nitrogen species and is observed when large amounts of peroxynitrite are produced. Right brain hemisphere sections from the mice overexpressing GFP showed strong parenchymal 3-NT

immunoreactivity (Figure 8, A and B) compared to sections obtained from mice overexpressing hNEP (Figure 8, C and D). The number of 3-NT immunoreactivity was reduced by 64% in both the cortex and hippocampus

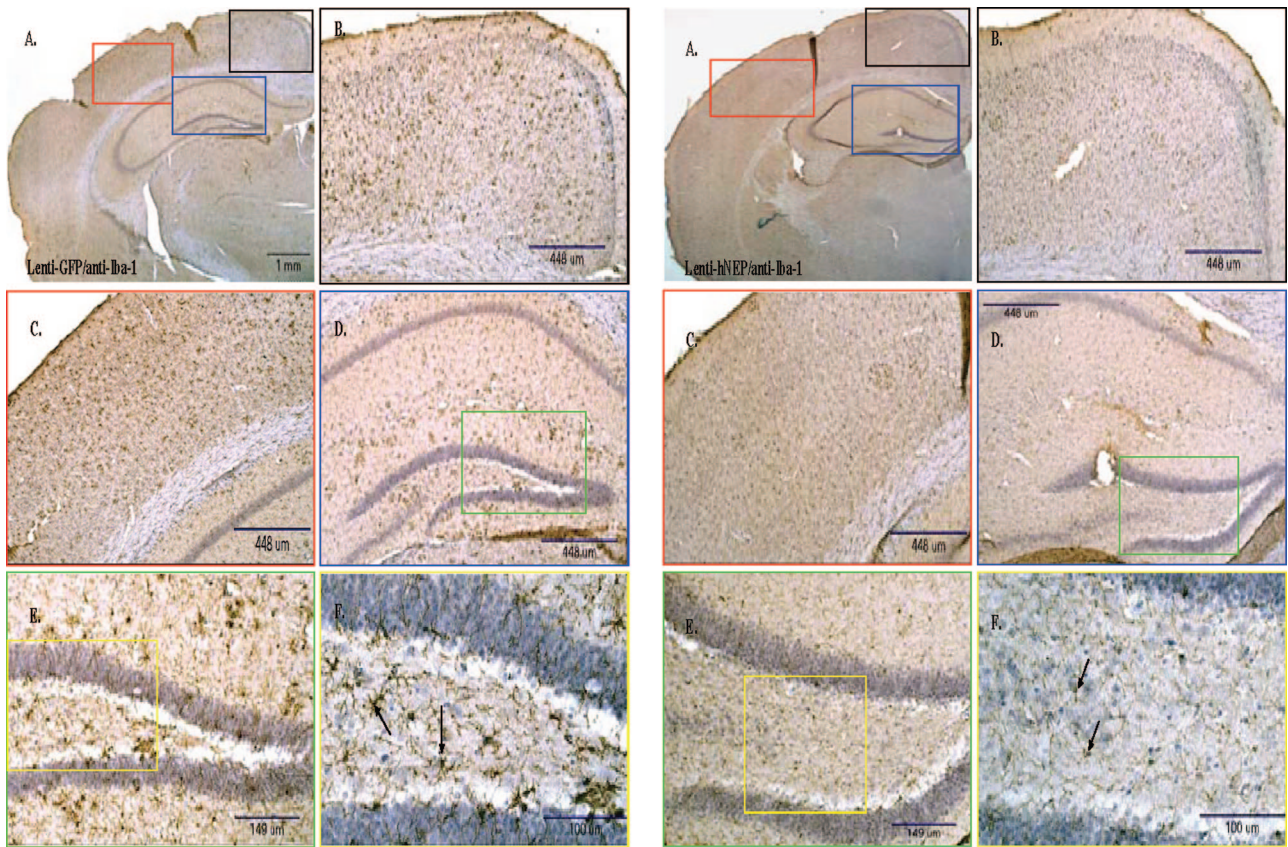


**Figure 6.** Density of Iba-1-positive microglial cells in APP/ΔPS1-Tg mouse brains after 4 months of Lenti-GFP or hNEP vectors injection. **A:** Right brain hemisphere sections of APP/ΔPS1-Tg mice overexpressing GFP (**A–F**) or hNEP (**G–L**) were immunostained with anti-mouse Iba-1 antibody (dilution 1:500; Wako Chemicals, Richmond, VA) to detect the distribution of activated microglial cells. The figures (**B–F**) and (**H–L**) represent an examination of **A** and **J**, respectively, at different parts and different magnification (**black, blue, red, green, and yellow boxes**) as indicated. **Black arrows** show examples of Iba-1-positive microglia.

(Figure 8, E and F) of mice treated with Lenti-hNEP compared to mice treated with Lenti-GFP. Most of the 3-NT staining was observed around the amyloid plaques, particularly in mouse brain hemispheres overexpressing GFP [Figure 8, B (white circles), G and H]. Furthermore, we analyzed the protein carbonyl content (a biomarker of reactive oxygen species) in the left brain hemisphere, and found that the level of oxidized proteins was less (~50%) in mice overexpressing hNEP than in mice overexpressing GFP (Figure 9, A–C).

#### *Overexpression of hNEP in APP/ΔPS1-Tg Mice Decreases the Memory Impairment*

APP/ΔPS1-Tg mice exhibit considerable amyloid plaque deposition at 6 to 8 months of age. Also they show signs of memory impairment at this age as it has been reported recently.<sup>27,28</sup> Therefore, 4 months after the injection of Lenti-hNEP and Lenti-GFP in the brain, mice were tested for spatial learning and memory retention using the Morris water maze test. This test has been used widely for investigating different aspects of learning and memory in mice and rodents (APP/ΔPS1-Tg mice at 3 and 8 months are shown in Figure 10A). On the 4th day of training and before removing the hidden platform, each group of mice overexpressing hNEP or GFP was tested for the spatial

learning ability; ie, escape latency and total distance traveled by mice to reach the platform in the presence of distal visual cues outside the swimming pool. The group of mice overexpressing hNEP showed a significantly enhanced spatial learning ability compared to that overexpressing GFP (Figure 10, B and C). The escape latency and average distance were  $12.77 \pm 1.26$  inches and  $64.04 \pm 9.07$  inches for the mice overexpressing hNEP, respectively. For the mice overexpressing GFP, the escape latency and average distance were  $21.08 \pm 3.98$  inches and  $103.9 \pm 17.20$  inches, respectively. In addition, in the spatial probe (memory retention) trial, in the absence of platform, the mice overexpressing hNEP showed significantly less cognitive impairment (better memory retention) compared to mice overexpressing GFP (Figure 10, D and E). In particular, the percentage of time spent in the NE quadrant by mice overexpressing hNEP was  $28.70 \pm 3.01$  seconds compared to  $18.74 \pm 3.27$  seconds spent by mice overexpressing GFP. In addition, the time percentage spent by both groups of mice overexpressing hNEP or GFP in the outer annular area were  $24.44 \pm 5.01$  seconds and  $45.14 \pm 7.07$  seconds, respectively. This significant difference in thigmotaxic behavior (ie, the innate nature of animals to hide in sheltered areas) between the two groups of mice indicates that hNEP mice were better able to navigate in the



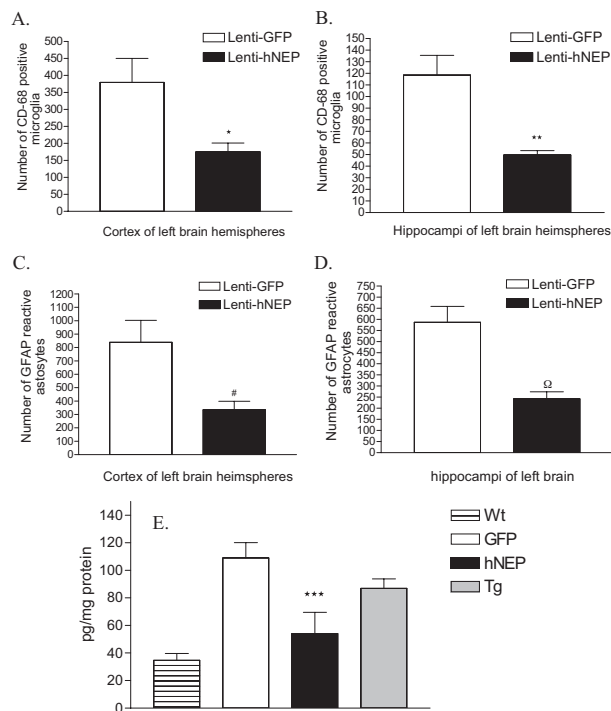


**Figure 7.** Quantitative analysis of activated microglia, astrocytes, and IL-6 in the brain of APP/ΔPS1-Tg mice after 4 months of hNEP or GFP overexpression. Brain sections from APP/ΔPS1-Tg mice overexpressing GFP or hNEP were stained with anti-mouse CD68 antibody to detect the activated microglial cells. Five sections of each mouse (around the injection site) were counted and averaged for the number of CD68-activated microglia in the cortex (A) and hippocampus (B) (\**P* = 0.0232, \*\**P* = 0.0066). C and D: Brain sections from APP/ΔPS1-Tg mice overexpressing GFP or hNEP were immunostained with anti-mouse GFAP antibody to detect the activated astrocytes. Five sections of each mouse (around the injection site) were counted and averaged for the number of GFAP-activated astrocytes in the cortex (A) and hippocampus (B) (#*P* = 0.0093, Ω*P* = 0.0016). E: Homogenized extracts from left brain hemispheres obtained from wild-type (C57BL/6) mice (Wt), non-treated APP/ΔPS1-Tg mice (7 months old) (Tg), and APP/ΔPS1-Tg mice overexpressing hNEP (hNEP), or GFP (GFP) were tested for IL-6 levels by the IL-6 ELISA kit (\*\*\**P* = 0.0017).

Morris water maze test by using learned visual cues and, thus, had better retention (memory) of spatial learning compared to mice overexpressing GFP.

### Discussion

NEP is one of the major Aβ peptide-degrading enzymes in the brain.<sup>5,6,31</sup> To date, several studies have shown that NEP is reduced in brain regions that are vulnerable to Aβ peptide accumulation, such as the hippocampus and associated cortices in AD.<sup>17,19,20</sup> We and others reported that overexpression of NEP in the brain of aged AD animal models as via gene therapy resulted in the reduction of amyloid load.<sup>23,32</sup> In addition, it has been shown that transgenic or cell-grafting overexpression of NEP prevented amyloid deposition.<sup>33,34</sup> However, the effect of

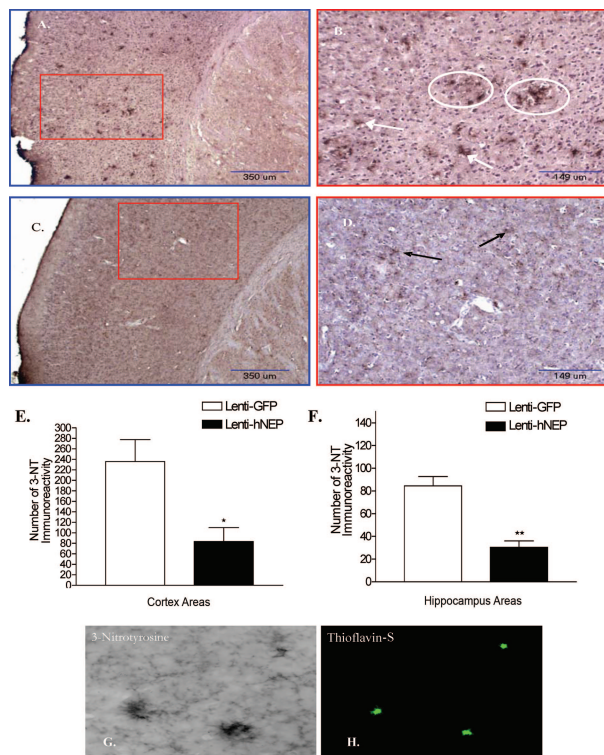


**Figure 8.** Oxidative stress assessment in the brain of APP/ΔPS1-Tg mice after 4 months of viral injection. Brain sections from APP/ΔPS1-Tg mice overexpressing GFP (A and B) or hNEP (C and D) were immunostained with anti-3-NT antibody. A and C were examined under different magnification (B and D) (red boxes) as indicated. Arrows indicate the 3-NT immunoreactivity, whereas white circles represent 3-NT immunoreactivity around the amyloid plaques. E and F: Five sections of each mouse (around the injection site) were counted and averaged for the number of 3-NT immunoreactivity in the cortex (E) and hippocampus (F) (\**P* = 0.0229, \*\**P* = 0.0092). G and H: Co-localization of amyloid plaques and 3-NT, brain sections of APP/ΔPS1-Tg mice overexpressing GFP, were immunostained with anti-3NT antibody (G), and double stained with the fluorescent amyloid stain thioflavin-S (H).

NEP lentiviral overexpression in the brain before the deposition of Aβ plaques is yet to be determined. Therefore, in this study, we investigated the effect of hNEP overexpression on reducing Aβ peptide accumulation in the brain of young APP/ΔPS1 transgenic mice. In addition, we investigated the effects of the hNEP-mediated reduction in Aβ peptide accumulation and amyloid load on inflammation, oxidative stress, and memory impairment. We found that overexpression of hNEP in the cortex-hippocampal area of 3-month-old APP/ΔPS1-Tg mice attenuated the number of amyloid plaques by 50% at 7 months compared to mice overexpressing GFP. This was most likely attributable to the reduction in Aβ peptide levels (Aβ<sub>1-40</sub> and Aβ<sub>1-42</sub>) hNEP-mediated (Figure 4, A-E). Because the lentiviruses were injected only into one region of the brain, and a reduction in Aβ peptide levels and amyloid deposits was seen in other regions of the brain as well, our observations suggest that a modest

**Table 2.** IL-6 Levels in APP/ΔPS1 Bitransgenic Mice after Lentiviral Injection

	Wt	GFP	hNEP	Tg
IL-6 (pg/mg protein)	34.64 ± 5.068	109.1 ± 11.08	54.10 ± 15.49	86.92 ± 6.902

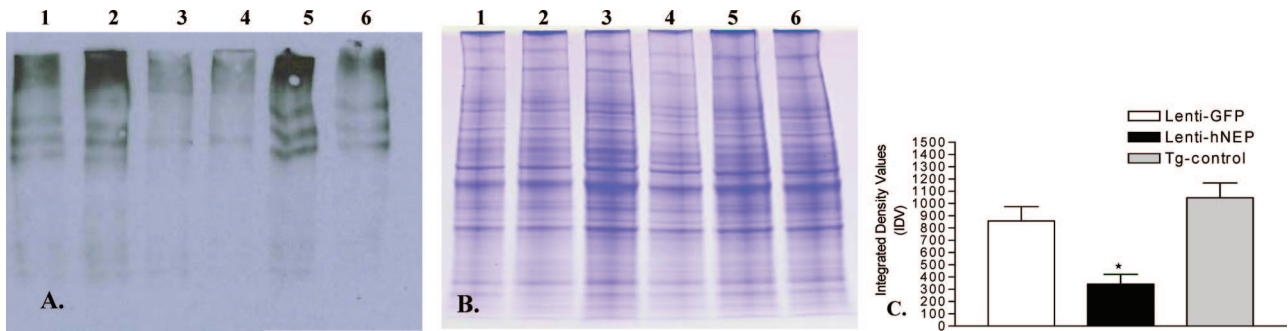


**Figure 9.** Carbonyl protein content in the brain of APP/ $\Delta$ PS1-Tg mice overexpressing hNEP and control. **A:** Extracts of left brain hemisphere obtained from mice overexpressing GFP (lanes 1 and 2), hNEP (lanes 3 and 4), as well as noninjected APP/ $\Delta$ PS1-Tg mice of the same age (Tg-control) (lanes 5 and 6) were analyzed for the level of oxidized proteins by Oxyblot and Western blot assays. **B:** Protein concentrations of samples used in **A** were run under similar conditions on sodium dodecyl sulfate-polyacrylamide gel electrophoresis and identified by Coomassie blue staining to control for loading differences between samples. **C:** Densitometry measurements of development of oxidized protein bands on Western blots were made using NIH image software (ImageJ 1.36b) and assigned as arbitrary integrated density values (IDV) (\* $P = 0.0390$  compared to Lenti-GFP or Tg-control IDV).

increase in NEP expression or activity in one part of the brain may have a significant effect on reducing the A $\beta$  peptide accumulation in the entire brain. The effect at a distance of NEP overexpression on the clearance of A $\beta$  peptide in the brain and body fluids was also reported elsewhere.<sup>35,36</sup> Disruption of NEP in mice resulted in

increased A $\beta$  peptide in the whole brain and plasma. Moreover, NEP has a high affinity toward A $\beta$  peptide compared to other small neuropeptides<sup>10,31,35</sup> and, in the AD brain, up-regulation of NEP activity will be mostly directed to degrade excess A $\beta$  peptide. Thus, gene therapy of NEP represents a potential therapeutic approach for AD.

NEP overexpression in the brain has been reported to be well tolerated by mice.<sup>33</sup> In the present study, the NEP gene transfer resulted in at least 4 months of hNEP expression in the brain and it will be necessary to determine how long this expression lasts and the effects of its long-term overexpression. Thus, it is necessary to characterize such gene transfer in different animal models, especially in those more relevant to humans, such as nonhuman primates.

Inflammation and oxidative stress have been linked to a number of age-related diseases including AD. These acute-phase processes are mediated by activated microglia and astrocytes that release an array of neurotoxic/inflammatory mediators such as cytokines and free radicals that contribute directly or indirectly to the degeneration of neurons.<sup>4,37-41</sup> This hypothesis is supported by the fact that senile plaques appear to be the site of inflammatory and oxidative stress processes, as evidenced by the presence of reactive microglia and astrocytes in and around these plaques,<sup>38,42</sup> and A $\beta$  peptide has been shown to activate both cells.<sup>40,43,44</sup> In fact, nearly all of the proinflammatory markers that have been studied in AD, including IL-1 $\beta$ , IL-6, and tumor necrosis factor- $\alpha$ , seem to be up-regulated in AD compared with control individuals,<sup>45,46</sup> and IL-6 has been reported to inhibit long-term potentiation both in mice and rats.<sup>47,48</sup> Among the indices of oxidative stress in AD brain are protein nitrotyrosylation and carbonylation, which are the markers of protein oxidation. On activation, glia cells can damage or kill neurons by generating nitrogen species such as nitric oxide<sup>49-52</sup> and peroxynitrite.<sup>53</sup> Peroxynitrite (formed from nitric oxide and superoxide radicals<sup>54</sup>) can both mediate DNA fragmentation by oxidative damage and prevent protein phosphorylation by tyrosine nitration, thus interfering with signal transduction mediated by tyrosine kinases. Thus, peroxynitrite

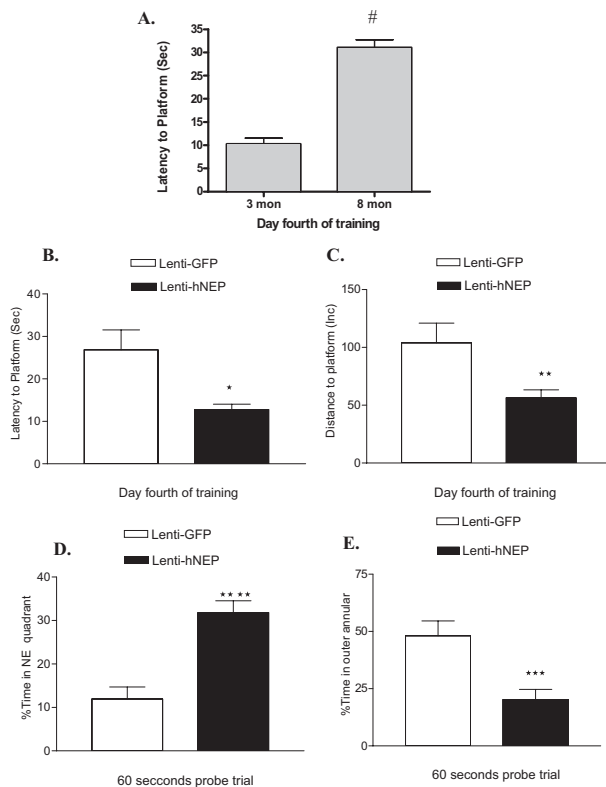


**Figure 10.** Morris water maze analysis. **A:** Memory impairment comparison of APP/ $\Delta$ PS1-Tg mice at 3 and 8 months (mon) of age ( $P < 0.001$ ). **B** and **C:** Each group of mice overexpressing hNEP (Lenti-hNEP) or GFP (Lenti-GFP) were tested on the 4th day of training for spatial learning (**B**) and memory retention (**D** and **E**). To test the mice for spatial learning, the escape latency (**B**), and total distance (**C**) taken by both groups of mice to reach the hidden platform were measured. To test for memory impairment (working memory retention), both groups of mice were tested for the percentage of time spent in the NE quadrant (**D**) and the percentage of time spent in the outer annular (around the wall of the tank) after the hidden platform was removed (\* $P = 0.0031$ , \*\* $P = 0.0077$ , \*\*\* $P = 0.0013$ , \*\*\*\* $P < 0.0001$ ). Morris water maze analysis was accomplished by the SMART video tracking system.

appears as a strong player in neuronal cell death in AD.<sup>55,56</sup> Indeed, 3-nitrotyrosine (3-NT), a marker for the presence of peroxynitrite, has been reported to be elevated five- to eightfold more in AD patients than in cognitively normal patients.<sup>57,58</sup> Moreover, peroxynitrite has been implicated in A $\beta$  peptide mediated N-methyl-D-aspartate receptor excitotoxic damage.<sup>59</sup> On the other hand, carbonyl derivatives are formed by reactive oxygen species-mediated oxidation of side chains of some amino acid residues. Protein oxidation often converts proteins to forms that are more susceptible to proteinases and, therefore, promotes their degradation by proteolysis.<sup>60</sup> Conversely, interactions of proteins with reactive oxygen species play controlling roles in cellular signaling, which affect cell remodeling, growth, and death.<sup>61,62</sup> Therefore, alterations in the rate of production and removal of oxidized proteins may contribute to the accumulation and damaging actions of oxidized proteins in normal and pathological aging.<sup>63,64</sup> Hence, increased reactive nitrogen and oxygen species production and oxidative modification of brain proteins may affect cellular functions and, eventually, lead to neuronal death in AD. Therefore, we investigated the affect of reducing amyloid load by hNEP on the inflammatory and oxidative stress level.

To examine how glial cells respond to A $\beta$  peptide clearance by hNEP, we correlated the cerebral level of A $\beta$  peptide with the density and number of activated CD68 microglia and GFAP astrocytes in the contralateral brain hemispheres of hNEP- or GFP-treated mice. Both cells were reduced in density and number by >50% in the right brain hemisphere of mice that overexpressed hNEP (Figure 7, A–D) compared to mice that overexpressed GFP. This parallel reduction of amyloid level and activated glial cells is consistent with our observation that 3-month-old APP/ $\Delta$ PS1-Tg mice display less amyloid plaque deposition in the cortex area (Figure 1, A–D) and, consequently, smaller numbers of GFAP-reactive astrocytes can be detected in that region along the hippocampus area (data not shown), whereas there is no presence of the CD68-activated microglial cells (data not shown). It is noteworthy that astrocytes are the predominant type of glial cell in the central nervous system and, probably, the first cell type to encounter and respond to A $\beta$  peptide accumulation. Thus, A $\beta$  peptide first activates the astrocytes that, in turn, lead to activation of microglia. These results are consistent with previous data showing in a mouse model of AD, that amyloid plaque-related astrogliosis was reduced as a result of increased NEP expression in mice injected unilaterally in the brain with fibrillar form of A $\beta$ <sub>1-42</sub> peptide.<sup>65</sup> Thus, our findings suggest that amyloid load has a direct impact on the inflammatory changes found in the brain of APP/ $\Delta$ PS1-Tg mice consistent with the amyloid cascade hypothesis. Moreover, the reduction of inflammatory processes was not restricted to the right brain hemisphere where hNEP overexpression occurred but was also observed in the left brain hemisphere. We found that IL-6 was reduced by 51% in the ipsilateral brain side of hNEP overexpression compared to that of mice that overexpressed GFP (Figure 7E). Although the reduction of total A $\beta$  peptide was <50% in the

left brain hemispheres (33% and 40% for A $\beta$ <sub>1-40</sub> and A $\beta$ <sub>1-42</sub>, respectively), the reduction of IL-6 by >50% could be attributed not only to decreased production of IL-6 from glial cells, but also to its decreased production from vascular endothelial cells. Because this mouse model of AD has been reported to develop cerebral amyloid angiopathy at ~7 months of age,<sup>66</sup> loss of NEP function would promote cerebral amyloid angiopathy.<sup>35</sup> Likewise, these results are in agreement with clinical studies, which suggest that nonsteroidal anti-inflammatory drugs, such as those used in arthritis, may delay or slow the progression of AD.<sup>45,46</sup> However, a major impediment to using of this class of drugs for treatment of AD is the number of serious side effects associated with the chronic use of nonsteroidal anti-inflammatory drugs such as gastric bleeding, heart attack, and stroke. Moreover, people 65 years and older are at high risk of developing these serious complications. Thus, NEP gene therapy seems to be a better treatment for AD.

In this study, we also investigated the influence of clearing A $\beta$  peptide and decreasing the amyloid load in APP/ $\Delta$ PS1-Tg mouse brains on the oxidative stress levels by measuring oxidized proteins. We found that mice that overexpressed hNEP for 4 months in the right brain hemisphere had 64% less 3-NT immunoreactivity (Figure 8, E and F) compared to mice that overexpressed GFP. In addition, 3-NT immunoreactivity showed strong co-localization with the amyloid plaques, which was apparent in the mice that overexpressed GFP compared to mice overexpressing hNEP [Figure 8, D (white circles), G, and H]. In the same context, we also found that the carbonyl protein content was less (~50%) in left brain hemispheres of mice that overexpressed hNEP than that of control mice (Figure 9, A–C). These findings suggest that the amyloid accumulation and deposition precede the oxidative stress in the brain, which is consistent with the amyloid cascade hypothesis. These results also support the assumption that reactive oxygen and nitrogen intermediates play a vital role in the pathogenesis and progression of AD. Furthermore, although the reduction of total A $\beta$  peptide concentration and attenuation of amyloid plaque deposition led to reduction of oxidative stress in the brain, the key form of A $\beta$  peptide that results in the induction of such response is still to be determined. Our data are in agreement with the *in vitro* studies showing that both the monomeric<sup>67</sup> and fibrillar<sup>68</sup> forms of A $\beta$  peptide play an important role in activating glial cells and producing oxidative stress responses.

Thus far, several reports have indicated that decreasing the accumulation of A $\beta$  peptide in the brain could prevent or reduce AD pathology and improve behavioral deficits.<sup>69–73</sup> On the other hand, continuous inhibition of NEP in the hippocampus by thiorphan<sup>21,22</sup> or NEP genetic deficiency led to increased A $\beta$  peptide accumulation and memory impairment. In this study we found that NEP gene therapy at an early stage of AD reduced the memory impairment by ~50%. Interestingly, the behavioral data showed that the APP/ $\Delta$ PS1-Tg mice spend more time circling the pool indicating a lack of spatial orientation. When the APP/ $\Delta$ PS1-Tg mice were treated with NEP lentiviruses there was a significant decrease in

the circling behavior suggesting an improvement in the spatial orientation. Our results are consistent with recently published studies<sup>33,74</sup> reporting that NEP/APP double-transgenic mice showed a reduction in amyloid load in the brain of aged mice, reduction in glial cells, and an improved Morris water maze memory performance. Thus, these data collectively confirm the importance of A $\beta$  peptide-lowering strategies at early stages of the disease to prevent the A $\beta$  peptide-related cognitive decline.

## References

- Khachaturian ZS: Diagnosis of Alzheimer's disease. *Arch Neurol* 1985, 42:1097-1105
- Braak H, Braak E: Morphological criteria for the recognition of Alzheimer's disease and the distribution pattern of cortical changes related to this disorder. *Neurobiol Aging* 1994, 3: 355-380
- Selkoe DJ: Alzheimer's disease: genes, proteins, and therapy. *Physiol Rev* 2001, 81:741-766
- Selkoe DJ: Alzheimer's disease is a synaptic failure. *Science* 2002, 298:789-791
- Iwata N, Tsubuki S, Takaki Y, Watanabe K, Sekiguchi M, Hosoki E, Kawashima-Morishima M, Lee H-J, Hama E, Sekine-Aizawa Y, Saido TC: Identification of the major A $\beta$ <sub>1-42</sub>-degrading catabolic pathway in brain parenchyma: suppression leads to biochemical and pathological deposition. *Nat Med* 2000, 6:143-150
- Iwata N, Tsubuki S, Takaki Y, Shirotani K, Lu B, Gerard NP, Gerard C, Hama E, Lee H-J, Saido TC: Metabolic regulation of brain A $\beta$  by neprilysin. *Science* 2001, 292:1550-1552
- Kerr MA, Kenny AJ: The purification and specificity of a neutral endopeptidase from rabbit kidney brush border. *Biochem J* 1974, 137:477-488
- Roques BP, Fournie-Zaluski MC, Soroca E, Lecomte JM, Malfroy B, Llorens C, Schwartz JC: The enkephalinase inhibitor thiorphan shows antinociceptive activity in mice. *Nature* 1980, 288:286-288
- Kenny AJ: Regulatory peptide metabolism at cell surfaces: the key role of endopeptidase-24.11. *Biomed Biochim Acta* 1986, 45:1503-1513
- Matsas R, Kenny AJ, Turner AJ: The metabolism of neuropeptides. The hydrolysis of peptides, including enkephalins, tachykinins and their analogues, by endopeptidase-24.11. *Biochem J* 1984, 223: 433-440
- Kanemitsu H, Tomiyama T, Mori H: Human neprilysin is capable of degrading amyloid  $\beta$  peptide not only in the monomeric form but also the pathological oligomeric form. *Neurosci Lett* 2003, 350:113-116
- El-Amouri SS, Zhu H, Yu J, Gage FH, Verma IM, Kindy MS: Nepriylsin protects neurons against Abeta peptide toxicity. *Brain Res* 2007, 1152:191-200
- Walsh DM, Townsend M, Podlisny MB, Shankar GM, Fadeeva JV, Agnaf OE, Hartley DM, Selkoe DJ: Certain inhibitors of synthetic amyloid beta-peptide (Abeta) fibrillogenesis block oligomerization of natural Abeta and thereby rescue long-term potentiation. *J Neurosci* 2005, 25:2455-2462
- Klyubin I, Walsh DM, Lemere CA, Cullen WK, Shankar GM, Betts V, Spooner ET, Jiang L, Anwyl R, Selkoe DJ, Rowan MJ: Amyloid beta protein immunotherapy neutralizes Abeta oligomers that disrupt synaptic plasticity in vivo. *Nat Med* 2005, 11:556-561
- Huang SM, Mouri A, Kokubo H, Nakajima R, Suemoto T, Higuchi M, Staufenbiel M, Noda Y, Yamaguchi H, Nabeshima T, Saido TC, Iwata N: Nepriylsin-sensitive synapse-associated amyloid-beta peptide oligomers impair neuronal plasticity and cognitive function. *J Biol Chem* 2006, 281:17941-17951
- Kirkitadze MD, Bitan G, Teplow DB: Paradigm shifts in Alzheimer's disease and other neurodegenerative disorders: the emerging role of oligomeric assemblies. *J Neurosci Res* 2002, 69:567-577
- Yasojima K, McGeer EG, McGeer PL: Relationship between beta amyloid peptide generating molecules and neprilysin in Alzheimer disease and normal brain. *Brain Res* 2001, 919:115-121
- Wang DS, Iwata N, Hama E, Saido TC, Dickson DW: Oxidized neprilysin in aging and Alzheimer's disease brains. *Biochem Biophys Res Commun* 2003, 310:236-241
- Caccamo A, Oddo S, Sugarman MC, Akbari Y, LaFerla FM: Age- and region-dependent alterations in Abeta-degrading enzymes: implications for Abeta-induced disorders. *Neurobiol Aging* 2005, 26:645-654
- Iwata N, Takaki Y, Fukami S, Tsubuki S, Saido TC: Region-specific reduction of A beta-degrading endopeptidase, neprilysin, in mouse hippocampus upon aging. *J Neurosci Res* 2002, 70:493-500
- Zou LB, Mouri A, Iwata N, Saido TC, Wang D, Wang MW, Mizoguchi H, Noda Y, Nabeshima T: Inhibition of neprilysin by infusion of thiorphan into the hippocampus causes an accumulation of amyloid beta and impairment of learning and memory. *J Pharmacol Exp Ther* 2006, 317:334-340
- Mouri A, Zou LB, Iwata N, Saido TC, Wang D, Wang MW, Noda Y, Nabeshima T: Inhibition of neprilysin by thiorphan (i.c.v.) causes an accumulation of amyloid beta and impairment of learning and memory. *Behav Brain Res* 2006, 168:83-91
- Marr RA, Rockenstein E, Mukherjee A, Kindy MS, Hersh LB, Gage FH, Verma IM, Masliah E: Nepriylsin gene transfer reduces human amyloid pathology in transgenic mice. *J Neurosci* 2003, 23:1992-1996
- Miyoshi H, Blomer U, Takahashi M, Gage FH, Verma IM: Development of a self-inactivating lentivirus vector. *J Virol* 1998, 72: 8150-8157
- Dull T, Zufferey R, Kelly M, Mandel RJ, Nguyen M, Trono D, Naldini L: A third-generation lentivirus vector with a conditional packaging system. *J Virol* 1998, 72:8463-8471
- Jankowsky JL, Fadale DJ, Anderson J, Xu GM, Gonzales V, Jenkins NA, Copeland NG, Lee MK, Younkin LH, Wagner SL, Younkin SG, Borchelt DR: Mutant presenilins specifically elevate the levels of the 42 residue beta-amyloid peptide in vivo: evidence for augmentation of a 42-specific gamma secretase. *Hum Mol Genet* 2004, 13:159-170
- Savonenko A, Xu GM, Melnikova T, Morton JL, Gonzales V, Wong MP, Price DL, Tang F, Markowska AL, Borchelt DR: Episodic-like memory deficits in the APP<sup>swE</sup>/PS1<sup>dE9</sup> mouse model of Alzheimer's disease: relationships to beta-amyloid deposition and neurotransmitter abnormalities. *Neurobiol Dis* 2005, 18:602-617
- Reiserer RS, Harrison FE, Syverud DC, McDonald MP: Impaired spatial learning in the APP<sup>swE</sup> + PSEN1<sup>DeltaE9</sup> bigenic mouse model of Alzheimer's disease. *Genes Brain Behav* 2007, 6:54-65
- Ito D, Tanaka K, Suzuki S, Dembo T, Fukuuchi Y: Enhanced expression of Iba1, ionized calcium-binding adapter molecule 1, after transient focal cerebral ischemia in rat brain. *Stroke* 2001, 32:1208-1215
- Fan R, Xu F, Previti ML, Davis J, Grande AM, Robinson JK, Van Nostrand WE: Minocycline reduces microglial activation and improves behavioral deficits in a transgenic model of cerebral microvascular amyloid. *J Neurosci* 2007, 27:3057-3063
- Iwata N, Higuchi M, Saido TC: Metabolism of amyloid-beta peptide and Alzheimer's disease. *Pharmacol Ther* 2005, 108:129-148
- Iwata N, Mizukami H, Shirotani K, Takaki Y, Muramatsu S, Lu B, Gerard NP, Gerard C, Ozawa K, Saido TC: Presynaptic localization of neprilysin contributes to efficient clearance of amyloid-beta peptide in mouse brain. *J Neurosci* 2004, 24:991-998
- Leissring MA, Farris W, Chang AY, Walsh DM, Wu X, Sun X, Frosch MP, Selkoe DJ: Enhanced proteolysis of beta-amyloid in APP transgenic mice prevents plaque formation, secondary pathology, and premature death. *Neuron* 2003, 40:1087-1093
- Hemming ML, Patterson M, Reske-Nielsen C, Lin L, Isacson O, Selkoe DJ: Reducing amyloid plaque burden via ex vivo gene delivery of an Abeta-degrading protease: a novel therapeutic approach to Alzheimer disease. *PLoS Med* 2007, 4:1405-1416
- Farris W, Schutz SG, Cirrito JR, Shankar GM, Sun X, George A, Leissring MA, Walsh DM, Qiu WQ, Holtzman DM, Selkoe DJ: Loss of neprilysin function promotes amyloid plaque formation and causes cerebral amyloid angiopathy. *Am J Pathol* 2007, 171:241-251
- Shirotani K, Tsubuki S, Iwata N, Takaki Y, Harigaya W, Maruyama K, Kiryu-Seo S, Kiyama H, Iwata H, Tomita T, Iwatsubo T, Saido TC: Nepriylsin degrades both amyloid beta peptides 1-40 and 1-42 most rapidly and efficiently among thiorphan- and phosphoramidon-sensitive endopeptidases. *J Biol Chem* 2001, 276:21895-21901
- Apelt J, Schliebs R: Beta-amyloid-induced glial expression of both pro- and anti-inflammatory cytokines in cerebral cortex of aged transgenic Tg2576 mice with Alzheimer plaque pathology. *Brain Res* 2001, 894:21-30

38. Itagaki S, McGeer PL, Akiyama H, Zhu S, Selkoe D: Relationship of microglia and astrocytes to amyloid deposits of Alzheimer disease. *J Neuroimmunol* 1989, 24:173–182
39. Chao CC, Hu S, Sheng WS, Bu D, Bukrinsky MI, Peterson PK: Cytokine-stimulated astrocytes damage human neurons via a nitric oxide mechanism. *Glia* 1996, 16:276–284
40. Hu J, Akama KT, Krafft GA, Chromy BA, Van Eldik LJ: Amyloid-beta peptide activates cultured astrocytes: morphological alterations, cytokine induction and nitric oxide release. *Brain Res* 1998, 785:195–206
41. Johnstone M, Gearing AJ, Miller KM: A central role for astrocytes in the inflammatory response to beta-amyloid: chemokines, cytokines and reactive oxygen species are produced. *J Neuroimmunol* 1999, 93:182–193
42. Rogers J, Luber-Nardo J, Styren SD, Civin WH: Expression of immune system-associated antigens by cells of the human central nervous system: relationship to the pathology of Alzheimer's disease. *Neurobiol Aging* 1988, 9:339–349
43. Fiala M, Zhang L, Gan X, Sherry B, Taub D, Graves MC, Hama S, Way D, Weinand M, Witte M, Lorton D, Kuo YM, Roher AE: Amyloid-beta induces chemokine secretion and monocyte migration across a human blood-brain barrier model. *Mol Med* 1998, 4:480–489
44. Yates SL, Burgess LH, Kocsis-Angle J, Antal JM, Dority MD, Embury PB, Piotrkowski AM, Brunden KR: Amyloid and amylin fibrils induce increases in proinflammatory cytokine and chemokine production by THP-1 cells and murine microglia. *J Neurochem* 2000, 74:1017–1025
45. Akiyama H, Barger S, Barnum S, Bradt B, Bauer J, Cole GM, Cooper NR, Eikelenboom P, Emmerling M, Fiebich BL, Finch CE, Frautschy S, Griffin WS, Hampel H, Hull M, Landreth G, Lue L, Mrak R, Mackenzie IR, McGeer PL, O'Banion MK, Pachter J, Pasinetti G, Plata-Salaman C, Rogers J, Rydel R, Shen Y, Streit W, Strohmeyer R, Tooyama I, Van Muiswinkel FL, Veerhuis R, Walker D, Webster S, Wegrzyniak B, Wenk G, Wyss-Coray T: Inflammation and Alzheimer's disease. *Neurobiol Aging* 2000, 21:383–421
46. Akiyama H, Arai T, Kondo H, Tanno E, Haga C, Ikeda K: Cell mediators of inflammation in the Alzheimer disease brain. *Alzheimer Dis Assoc Disord* 2000, 14(Suppl 1):S47–S53
47. Bellingier FP, Madamba SG, Campbell IL, Siggins GR: Reduced long-term potentiation in the dentate gyrus of transgenic mice with cerebral overexpression of interleukin-6. *Neurosci Lett* 1995, 198:95–98
48. Li A-J, Katafuchi T, Oda S, Hori T, Oomura Y: Interleukin-6 inhibits long-term potentiation in rat hippocampal slices. *Brain Res* 1997, 748:30–38
49. Boje KM, Arora PK: Microglial-produced nitric oxide and reactive nitrogen oxides mediate neuronal cell death. *Brain Res* 1992, 587:250–256
50. Chao CC, Hu S, Molitor TW, Shaskan EG, Peterson PK: Activated microglia mediate neuronal cell injury via a nitric oxide mechanism. *J Immunol* 1992, 149:2736–2741
51. Hu S, Peterson PK, Chao CC: Cytokine-mediated neuronal apoptosis. *Neurochem Int* 1997, 30:427–431
52. Goodwin JL, Uemura E, Cunnick JE: Microglial release of nitric oxide by the synergistic action of beta-amyloid and IFN-gamma. *Brain Res* 1995, 692:207–214
53. Xie Z, Wei M, Morgan TE, Fabrizio P, Han D, Finch CE, Longo VD: Peroxynitrite mediates neurotoxicity of amyloid beta-peptide 1-42 and lipopolysaccharide-activated microglia. *J Neurosci* 2002, 22:3484–3492
54. Beckman JS: Oxidative damage and tyrosine nitration from peroxynitrite. *Chem Res Toxicol* 1996, 9:836–844
55. Good PF, Werner P, Hsu A, Olanow CW, Perl DP: Evidence of neuronal oxidative damage in Alzheimer's disease. *Am J Pathol* 1996, 149:21–28
56. Smith MA, Richey-Harris P, Sayre LM, Beckman JS, Perry G: Widespread peroxynitrite-mediated damage in Alzheimer's disease. *J Neurosci* 1997, 17:2653–2657
57. Beal MF: Oxidatively modified proteins in aging and disease. *Free Radic Biol Med* 2002, 32:797–803
58. Hensley K, Maidt ML, Yu Z, Sang H, Markesbery WR, Floyd RA: Electrochemical analysis of protein nitrotyrosine and dityrosine in the Alzheimer brain indicates region-specific accumulation. *J Neurosci* 1998, 18:8126–8132
59. Wang Q, Rowan MJ, Anwyl R: Beta-amyloid-mediated inhibition of NMDA receptor-dependent long-term potentiation induction involves activation of microglia and stimulation of inducible nitric oxide synthase and superoxide. *J Neurosci* 2004, 24:6049–6056
60. Stadtman ER: Metal ion-catalyzed oxidation of proteins: biochemical mechanisms and biological consequences. *Free Radic Biol Med* 1990, 9:315–325
61. Remacle J, Raes M, Toussaint O, Renard P, Rao G: Low levels of reactive oxygen species as modulators of cell function. *Mutat Res* 1995, 316:103–122
62. Kamata H, Hirata H: Redox regulation of cellular signalling. *Cell Signal* 1999, 11:1–14
63. Dean RT, Fu S, Stocker R, Davies MJ: Biochemistry and pathology of radical-mediated protein oxidation. *Biochem J* 1997, 324:1–18
64. Butterfield DA, Stadtman ER: Protein oxidation processes in aging brain. *Adv Cell Aging Gerontol* 1997, 2:161–191
65. Mohajeri MH, Wollmer MA, Nitsch RM: Abeta 42-induced increase in neprilysin is associated with prevention of amyloid plaque formation in vivo. *J Biol Chem* 2002, 277:35460–35465
66. Garcia-Alloza M, Robbins EM, Zhang-Nunes SX, Purcell SM, Betensky RA, Raju S, Prada C, Greenberg SM, Bacskai BJ, Frosch MP: Characterization of amyloid deposition in the APP<sup>swe</sup>/PS1<sup>dE9</sup> mouse model of Alzheimer disease. *Neurobiol Dis* 2006, 24:516–524
67. Li M, Sunamoto M, Ohnishi K, Ichimori Y: Beta-amyloid protein-dependent nitric oxide production from microglial cells and neurotoxicity. *Brain Res* 1996, 720:93–100
68. McDonald DR, Brunden KR, Landreth GE: Amyloid fibrils activate tyrosine kinase-dependent signaling and superoxide production in microglia. *J Neurosci* 1997, 17:2284–2294
69. Schenk D, Barbour R, Dunn W, Gordon G, Grajeda H, Guido T, Hu K, Huang J, Johnson-Wood K, Khan K, Kholodenko D, Lee M, Liao Z, Lieberburg I, Motter R, Mutter L, Soriano F, Shopp G, Vasquez N, Vandever C, Walker S, Wogulis M, Yednock T, Games D, Seubert P: Immunization with amyloid-beta attenuates Alzheimer-disease-like pathology in the PDAPP mouse. *Nature* 1999, 400:173–177
70. Janus C, Pearson J, McLaurin J, Mathews PM, Jiang Y, Schmidt SD, Chishti MA, Horne P, Heslin D, French J, Mount HT, Nixon RA, Mercken M, Bergeron C, Fraser PE, St George-Hyslop P, Westaway D: A beta peptide immunization reduces behavioural impairment and plaques in a model of Alzheimer's disease. *Nature* 2000, 408:979–982
71. Morgan D, Diamond DM, Gottschall PE, Ugen KE, Dickey C, Hardy J, Duff K, Jantzen P, DiCarlo G, Wilcock D, Connor K, Hatcher J, Hope C, Gordon M, Arendash GW: Aβ peptide vaccination prevents memory loss in an animal model of Alzheimer's disease. *Nature* 2000, 408:982–985
72. Hock C, Konietzko U, Streffer JR, Tracy J, Signorell A, Muller-Tillmanns B, Lemke U, Henke K, Moritz E, Garcia E, Wollmer MA, Umrbricht D, de Quervain DJ, Hofmann M, Maddalena A, Papassotiropoulos A, Nitsch RM: Antibodies against beta-amyloid slow cognitive decline in Alzheimer's disease. *Neuron* 2003, 38:547–554
73. Lazarov O, Robinson J, Tang YP, Hairston IS, Korade-Mirnics Z, Lee VM, Hersh LB, Sapolsky RM, Mirnics K, Sisodia SS: Environmental enrichment reduces Aβ levels and amyloid deposition in transgenic mice. *Cell* 2005, 120:701–713
74. Poirier R, Wolfert DP, Welzl H, Tracy J, Galsworthy MJ, Nitsch RM, Mohajeri MH: Neuronal neprilysin overexpression is associated with attenuation of Abeta-related spatial memory deficit. *Neurobiol Dis* 2006, 24:475–483